

PPPL-5334

Recent Advances in Stellarator Optimization

D. Gates, T. Brown, J. Breslau,
S. A. Lazerson, H. Mynick, G.H. Neilson, N. Pomphreys

December 2016



Prepared for the U.S. Department of Energy under Contract DE-AC02-09CH11466.

Princeton Plasma Physics Laboratory

Report Disclaimers

Full Legal Disclaimer

This report was prepared as an account of work sponsored by an agency of the United States Government. Neither the United States Government nor any agency thereof, nor any of their employees, nor any of their contractors, subcontractors or their employees, makes any warranty, express or implied, or assumes any legal liability or responsibility for the accuracy, completeness, or any third party's use or the results of such use of any information, apparatus, product, or process disclosed, or represents that its use would not infringe privately owned rights. Reference herein to any specific commercial product, process, or service by trade name, trademark, manufacturer, or otherwise, does not necessarily constitute or imply its endorsement, recommendation, or favoring by the United States Government or any agency thereof or its contractors or subcontractors. The views and opinions of authors expressed herein do not necessarily state or reflect those of the United States Government or any agency thereof.

Trademark Disclaimer

Reference herein to any specific commercial product, process, or service by trade name, trademark, manufacturer, or otherwise, does not necessarily constitute or imply its endorsement, recommendation, or favoring by the United States Government or any agency thereof or its contractors or subcontractors.

PPPL Report Availability

Princeton Plasma Physics Laboratory:

<http://www.pppl.gov/techreports.cfm>

Office of Scientific and Technical Information (OSTI):

<http://www.osti.gov/scitech/>

Related Links:

[U.S. Department of Energy](#)

[U.S. Department of Energy Office of Science](#)

[U.S. Department of Energy Office of Fusion Energy Sciences](#)

Recent Advances in Stellarator Optimization

D. A. Gates¹, A. H. Boozer², T. Brown¹, J. Breslau¹, D. Curreli³, M. Landreman⁴, S. A.

Lazerson¹, J. Lore⁵, H. Mynick¹, G.H. Neilson¹, N. Pomphrey¹, P. Xanthopoulos⁶

¹Princeton Plasma Physics Laboratory, Princeton, NJ 08543 ²Columbia University, New York,

NY 10027 ³U. Illinois Champaign-Urbana, Champaign, IL 61820 ⁴University of Maryland,

College Park, MD 20742 ⁵Oak Ridge National Laboratory, Oak Ridge, TN 37831 ⁶Max

Planck Institut-fur-Plasmaphysik, Greifswald, Germany

Abstract

Computational optimization has revolutionized the field of stellarator design. To date, optimizations have focused primarily on optimization of neoclassical confinement and ideal MHD stability, although limited optimization of other parameters has also been performed. One of the criticisms that has been leveled at existing methods of design is the complexity of the resultant field coils. Recently, a new coil optimization code - COILOPT++, which uses a spline instead of a Fourier representation of the coils, - was written and included in the STELLOPT suite of codes. The advantage of this method is that it allows the addition of real space constraints on the locations of the coils. The code has been tested by generating coil designs for optimized quasi-axisymmetric stellarator plasma configurations of different aspect ratios. As an initial exercise, a constraint that the windings be vertical was placed on large major radius half of the non-planar coils. Further constraints were also imposed that guaranteed that sector blanket modules could be removed from between the coils, enabling a sector maintenance scheme. Results of this exercise will be presented. New ideas on methods for the optimization of turbulent transport have garnered much attention since these methods have led to design concepts that are calculated to have reduced turbulent heat

loss. We have explored possibilities for generating an experimental database to test whether the reduction in transport that is predicted is consistent with experimental observations. To this end, a series of equilibria that can be made in the now latent QUASAR experiment have been identified that will test the predicted transport scalings. Fast particle confinement studies aimed at developing a generalized optimization algorithm are also discussed. A new algorithm developed for the design of the scraper element on W7-X is presented along with ideas for automating the optimization approach.

1. Introduction

The stellarator concept, like its symmetric cousin the tokamak, is a toroidal magnetic confinement device which holds promise for confining plasmas with sufficient efficiency to reach the plasma parameters required to generate fusion energy. Because stellarators use external magnets to generate nearly all the confining fields they are generally free of the plasma terminating instabilities frequently found in tokamaks. Additionally, the use of mostly-external fields for confinement obviates the need for external current drive for configuration sustainment, which is a major impediment to achieving steady state in a tokamak. Steady-state maintenance of the magnetic configuration provides additional advantages: 1) no possibility of the loss of positional equilibrium, which is associated with disruptions, and 2) no requirement to have a plasma current greater than 5MA, where the problem of runaway electrons becomes severe. An important property, which reduces the cost and time for fusion energy development, is that stellarator plasmas are subject to external control rather than being in a self-organized state. This removes many uncertainties in the extrapolation from smaller experiments to the reactor scale. In the early years of stellarator research energy confinement was severely limited by neoclassical ion losses, caused by the asymmetry associated with the 3D nature of the fields. However, be-

ginning in the 1980s, design concepts were developed that addressed neoclassical losses. The technique that was employed involved a conceptual change in the stellarator design process. Early stellarator designs were developed by first creating a coil set, and then, investigating the resultant plasma properties. In the new paradigm, a plasma equilibrium is designed to have (for example) good neoclassical confinement properties and then a coil set is designed to generate that equilibrium. The primary drivers for this new design paradigm were advances in theoretical understanding of the sources of the large neoclassical losses in traditional stellarator designs. Numerous publications on the topic of enhanced neoclassical stellarator confinement are very well summarized in Reference [1].

Of particular note are the references by Boozer which show 1) the guiding-center equations of motion in flux coordinates depend only on the magnitude of the magnetic field, and not on its individual components [2], and 2) that if two systems are both symmetric in flux coordinates, the orbits and transport coefficients in one system may be gotten from those of the other by a simple parameter mapping between the two [3], regardless of their physical shape. These ideas led shortly thereafter the first stellarator design based on the idea of “quasi-symmetry” [4].

Three types of stellarators appear to have the potential for reactors. (1) Quasi-Axisymmetric (QA), which in design space is continuous with the tokamak, (2) Quasi-Helical (QH), which tends to have better energetic particle confinement, and (3) Quasi-Omnigeneous (QO), which has properties that are essentially independent of the plasma pressure and can be designed to have no plasma current. Stellarators have approximately an order of magnitude more degrees of freedom in external magnetic fields than tokamaks in the number of externally produced magnetic field distributions that can be used for plasma control. The number of degrees of freedom is far too large to be explored empirically; design points must be chosen through well-organized

computations which exploit this freedom to address issues in fusion development. In addition to the optimization of neoclassical confinement the newest systems are also optimized relative to ideal MHD stability such that they are absolutely stable to all ideal MHD perturbations. The procedure for guaranteeing MHD stability is described in detail in Reference [5] and [6]. The capabilities for the neo-classical + MHD stability optimization are contained within the STELLOPT suite of codes which is described in detail in Reference [7].

This paper describes advances to the computational tools attempts to utilize these advances to demonstrate that major design improvements can be made in areas such as simplified coil designs, improved divertor options, better confinement of alpha particles to reduce damage to the chamber walls, and reduced micro-turbulent transport.

2. Areas for Improved Optimization Studies

Improved coil design: We show examples of the use of modernized coil design tools STELLOPT/COILOPT++ to address the issue of coil complexity in stellarators and also investigate the engineering feasibility of these designs.

Turbulent transport studies: We present a brief summary of an exciting new area for stellarator design - the optimization of turbulent transport. We also present an experimental strategy to test directly comparable theoretical predictions from the GENE code so as to place the concept of turbulent transport optimization on a sufficiently firm footing that it can be confidently used to design turbulence optimized configurations.

Fast particle optimization: We discuss capabilities to optimize the confinement of fast particles within the context of the simplified stellarator coil design tools STELLOPT/COILOPT++ described above.

Divertor Design: We describe a method to incorporate divertor plate design options into the STELLOPT code and incorporate useful engineering constraints into the design process.

2.1 Improved Coil Design

Dramatic improvements to the coil design features of the STELLOPT code, embodied in a new code called COILOPT++, have been used to develop coil designs that are compatible with a large sector maintenance scheme [8]. The process involves coupling explicit engineering constraints into the optimization, which was modified to operate with spline representation of the coils instead of Fourier modes. High-Tc superconducting tapes, which permit much higher current density and higher magnetic field than the conventional superconductors, while also providing much greater flexibility for the cooling systems hold promise for reducing the size of the coil windings. The new conductors offer additional unique advantages for non-axisymmetric plasmas. For example the minimum local radius of curvature is often a constraint for stellarator coils, but the increased current density in the new conductors enables coils to be thinner, relaxing the curvature constraint.

An $A = 6.0$ quasi-axisymmetric stellarator plasma was considered, based on the work of Ku and Boozer [9]. In moving from ARIES-CS parameters ($A=4.5$, $R = 7.75\text{m}$, $B = 5.7\text{T}$) to an aspect ratio $A=6.0$ configuration while retaining the values for fusion power, beta, plasma volume, and toroidal magnetic field leads to a major radius of 9.39m . The plasma current, I_p , is scaled to keep $I_p/RB_\phi = 0.045$, leading to $I_p = 2.6\text{MA}$. Plasma beta is set to be 4.0% . Fourier coefficients describing the target plasma boundary of the $A=6.0$ configuration are taken from Table 1 of reference [10], and scaled appropriately.

The resultant stellarator coil design with a large sector maintenance scheme is shown in Fig-

ure 1. The coil optimization was sufficiently successful with modular coils only, that it was not necessary to add trim coils, although the COILOPT++ code supports that possibility. Although two of the three modular coil shapes are planar at the outboard side, a free-boundary VMEC equilibrium supported by the coil set nonetheless has nearly as much rotational transform as the fixed-boundary equilibrium targeted by the coil optimization, as shown in figure 2. Figure 3 shows the normalized neoclassical transport ϵ_{eff} , computed using the NEO code of [12], which is found to be only slightly higher than in other optimized stellarators. We have also obtained a similar fixed-boundary equilibrium with lower ϵ_{eff} , though detailed coil optimizations have not yet been carried out for this configuration.

The ideas described in this section are the first attempt to include constraints on the physical location of the coils within the winding surface for an optimized stellarator. Given the ease with which an attractive solution was found, it seems clear that additional physical constraints could be added if it is deemed advantageous.

While a comprehensive nonlinear optimizer like COILOPT++ is needed for a detailed experimental design, increased distances between coils can also be achieved using the new fast and robust REGCOIL approach [13]. In REGCOIL, the problem of finding coil shapes while simultaneously maximizing the coil-coil distances is posed as a linear least-squares minimization, so the coil shapes are obtained by solving a single linear system with no iteration required. The convex formulation guarantees that the solution found is a global optimum and not just a local one. Due to this speed and robustness, REGCOIL is therefore well suited to rapidly scoping new stellarator configurations, and for targeting coil complexity within the fixed-boundary optimization of the plasma shape.

A second important aspect of stellarator coil complexity is the fact that stellarator coils typ-

ically need to be relatively close to the plasma, much more so than the coils in a tokamak. The reason for this small plasma-coil separation in stellarators is that the shaping components of the magnetic field created by coils decay through space, so for a given stellarator plasma shape, the non-planar excursions of modular coils must grow exponentially as the plasma-coil separation is increased. The issue of small plasma-coil separation becomes even more important in a reactor, because a blanket and neutron shielding must fit between the plasma and coils. Indeed, in the ARIES-CS reactor study, plasma-coil separation was identified as “the most influential parameter for the stellarator’s size and cost” [11]. However, the maximum feasible plasma-coil separation is a strong function of the plasma shape. For example, plasma shapes with concave regions tend to require very close coils, whereas plasma shapes with convex cross-sections permit the coils to be more distant. recently, Landreman and Boozer [14] defined and explored several new magnetic field “efficiency” metrics, called the efficiency sequence and feasibility sequence. These metrics can be used to define “efficient shapes” to help guide shape optimization which in turn can decrease the need for small plasma coil separation. Insight into this dependence of coil complexity on plasma shape and plasma-coil separation can be gained by drawing an analogy with tomographic inversion and image de-blurring. In all these contexts, one aims to solve a linear system $\overset{\leftrightarrow}{M}\vec{x} = \vec{b}$ for \vec{x} given some operator $\overset{\leftrightarrow}{M}$ that has a smoothing behavior [15]. In image de-blurring, \vec{b} is the blurred data, $\overset{\leftrightarrow}{M}$ is the blurring operation, and \vec{x} is the desired true image. In the stellarator case $-\vec{b}$ represents the component of the toroidal field normal to the desired outer magnetic surface which must be cancelled by shaping currents, and $\overset{\leftrightarrow}{M}$ is the Biot-Savart integral relating shaping currents \vec{x} on the coil winding surface to normal magnetic field on the desired plasma surface; see [14] for details. In all of these problems, the smoothing operator $\overset{\leftrightarrow}{M}$ has an arbitrarily large condition number (the ratio of largest to small-

est singular values), since smoothing strongly suppresses fine-scale structures, and this suppression corresponds to small singular values. Generally, in the singular value decomposition $\overset{\leftrightarrow}{M} = \overset{\leftrightarrow}{U} \overset{\leftrightarrow}{\Sigma} \overset{\leftrightarrow}{V}^T$ where $\overset{\leftrightarrow}{\Sigma} = \text{diag}(\vec{\sigma})$, the sequence of singular values $\vec{\sigma}$ is exponentially decreasing. The formal solution $\vec{x} = \overset{\leftrightarrow}{M}^{-1} \vec{b} = \overset{\leftrightarrow}{V} \overset{\leftrightarrow}{\Sigma}^{-1} \overset{\leftrightarrow}{U}^T \vec{b}$ tends to diverge since one multiplies by the inverse of the arbitrarily small singular values, corresponding to the fact that fine-scale components of the solution are effectively undetermined by the data \vec{b} . In tomographic inversion and image deblurring, the so-called ‘discrete Picard condition’ is the condition that the projection of the data onto the singular vectors, $\overset{\leftrightarrow}{U}^T \vec{b}$, decreases faster than the rate by which the singular values decrease [15]. A finite solution \vec{x} exists only if the discrete Picard condition is satisfied. We call $\overset{\leftrightarrow}{U}^T \vec{b}$ the ‘efficiency sequence’ and $\overset{\leftrightarrow}{\Sigma}^{-1} \overset{\leftrightarrow}{U}^T \vec{b}$ the ‘feasibility sequence’, so the discrete Picard condition is the condition that the feasibility sequence decreases rather than increases. Applications of the discrete Picard condition in tomography and image deblurring, with corresponding examples of the efficiency and feasibility sequences, can be found in [15, 16, 17, 18].

In the stellarator context, a given plasma shape can only be produced by coils on a given coil winding surface if the discrete Picard condition is satisfied. The efficiency sequence $\overset{\leftrightarrow}{U}^T \vec{b}$ is relatively insensitive to the plasma-coil separation but is a strong function of the plasma shape, with the sequence decreasing rapidly for convex shapes but decreasing slowly for concave shapes [14]. Conversely, the sequence of singular values is a weak function of plasma shape and a strong function of plasma-coil separation, decreasing more rapidly as the coils are further from the plasma. Thus, this analogy provides several lessons for stellarator design. First, for any given plasma shape and size, there is a fundamental limit to how far away the shaping coils can be, given by the distance at which the feasibility sequence changes from decreasing to increasing. Second, we should seek plasma shapes that have a rapidly decreasing efficiency

sequence. (Or nearly equivalently, we should seek plasma shapes that have a rapidly decreasing feasibility sequence for a given plasma-coil separation.) Such plasma shapes are then possible to produce using distant coils. The efficiency and feasibility sequences provide general insight into the difficulty of producing a given plasma shape without the need for a detailed coil optimization. Thus, it may be possible to use the efficiency or feasibility sequences to guide plasma shape optimization to decrease the need for small plasma coil separation.

2.2 Turbulent transport Studies

A major advancement for stellarator physics is the ability to simulate micro-turbulence driven by the radial gradient that the plasma pressure forms in the device. For such simulations, a well-established model, so-called “nonlinear gyrokinetics”, is usually implemented. Broadly speaking, this theory entails a reduced Lagrangian description, in that the fast gyration of charged particles is averaged out in the equations of motion. In addition, the averaging operation is also applied to Ampère’s law and Poisson’s equation for the calculation of the fields (vector and scalar potential, respectively). Based on this approach, a number of gyrokinetic codes has been developed over the last few years for the simulation of micro-turbulence in non-axisymmetric geometry, including GKV [19], GENE [20], and GS2 [21]. To complement cpu-intensive, peta-scale calculations, the theoretical understanding of instabilities in stellarators has also been pursued. Notable examples of this ongoing work is the prediction that a certain class of stellarators could be immune to turbulence induced by the trapped-particle (predominantly electron) population [22], or that most stellarators are intrinsically able to ameliorate strong ion temperature gradient (ITG) driven turbulence over the magnetic surface, caused locally by 3D shaping [23]. The experimental confirmation of these theoretical results has been planned for

the upcoming experimental campaigns of W7-X, and insights could be exploited towards the design of novel configurations with reduced turbulence.

Meanwhile, proof-of-principle work has already demonstrated the feasibility of “turbulence optimization”. Here, the main idea is to devise computationally efficient target functions which could appropriately capture the essential physics of micro-turbulence. These functions are embedded into the χ^2 function that STELLOPT seeks to minimize. Since direct simulations require a prohibitively large amount of time for an iterative scheme, target functions are constructed using simpler “proxies”, involving either geometric quantities (such as the curvature of the magnetic field or the distance between adjacent flux surfaces) or more sophisticated expressions based on mixing-length estimates for the heat flux [24, 25]. This methodology has been applied so far to QUASAR [26] as well as W7-X [27] suggesting that both these configurations can be modified to reduce turbulent transport, also without compromising the neoclassical optimization.

In order to validate such predictions of reduced ITG turbulence reduction in QUASAR, a set of six free boundary configurations with 2% beta but different values of the global magnetic shear was produced using the STELLOPT code (the corresponding iota profiles are shown in Figure 5). These, experimentally realizable in the QUASAR facility, configurations showed little variation in neoclassical transport, however the proxy used for ITG turbulence optimization indicated up to a factor of 2 reduction to the transport levels. Following this prediction, gyrokinetic calculations to appear in a future publication showed a significant reduction of ITG turbulence.

2.3 Energetic Ion Confinement

Any viable magnetic fusion reactor will need to confine alpha particles long enough for them to transfer most of their energy to the main species. Meeting this requirement is more challenging for nonaxisymmetric schemes than for axisymmetric ones. Axisymmetry implies conservation of canonical angular momentum, which implies that all particle trajectories are confined (within a poloidal gyroradius of a given magnetic surface) in the absence of collisions and turbulence. However in nonaxisymmetric plasmas, the absence of such a conservation law means that trapped particle trajectories are not necessarily confined. For thermal particles, the problem is mitigated by collisionless detrapping associated with poloidal ExB drift, but for fast particles this helpful process is weak due to the smaller ratio of ExB to parallel speed. The scale of the fast-particle confinement problem is clearly shown in [28], which found all trapped alpha particles to be lost in $\sim 10^{-4} - 10^{-3}s$ in simulations of a conventional (not optimized) $l = 2$ stellarator and of W7-AS. For comparison, the required alpha confinement time for typical reactor parameters can be estimated as $\geq 0.1s$. Fast particle confinement in modern optimized designs such as W7-X and NCSX is much improved compared to conventional stellarators [29], but remains one of the main challenges for the concept. For instance, alpha confinement remained one of the most serious concerns expressed in the ARIES-CS reactor study [30]. Even though the ARIES design was able to reduce alpha losses to 5% over a slowing-down time. Neoclassical optimization naturally leads to improvement in the confinement of fast particles, but while confinement of thermal and fast particles is related, some considerations are different. Targets for neoclassical optimization (e.g. effective helical ripple, [12]) are typically derived using a “radially local” analysis, in which an expansion is made in the smallness of the particle orbit width compared to equilibrium scale lengths. For fast particles, this ratio is often not small, so the finite orbit width must be taken into account. Moreover, alpha particles are likely

to be born close to the magnetic axis, making finite-orbit-width effects especially important. Also, neoclassical transport computations assume a nearly Maxwellian distribution function, whereas the fast particle distribution function is often very far from Maxwellian. Collisions are central to neoclassical confinement but unimportant for fast-particle confinement, whereas the opposite is often true for poloidal magnetic drift. Thus, separate figures of merit for fast particle confinement should ideally be included in stellarator optimization in addition to the neoclassical targets that have been used to date.

Given improvements in computing power, as well as code development efforts in the past year, it is more feasible than ever before to directly optimize the confinement of fast particle trajectories. STELLOPT has recently been coupled to the gyro-center following parts of the BEAMS3D code [31] allowing massively parallel computations. Initial tests have been carried out using this pair of codes on as many as 10,000 processors on the Hydra supercomputer in Garching, Germany [32]. In this work 12,000 particles were followed until losses appeared to reach an asymptote (approximately a slowing down time, see Figure 6). Losses for this case were dominated by particles with small pitch angles (large perpendicular energies). These computations also indicated the need for fast proxies if computations are to be carried out using more modest computational resources. Thus development of proxy functions for energetic particle confinement may still play a key role in energetic particle confinement optimization.

More specifically one may ask what qualities of a stellarator result in improved energetic particle confinement? Examining the optimization performed using the BEAMS3D coupling to STELLOPT it can be shown that low order toroidal modes played the dominant role in improving confinement (see Figure 7). Confinement appears to be extremely sensitive to low order toroidal modes in the collisionless limit. Thus optimizing energetic particle confinement in

stellarators may require a careful tradeoff between neoclassical and energetic particle confinement. However, the full nature of energetic particle confinement is more complex than these simulations suggest.

The interaction of energetic particles with Alfvén instabilities is an important topic in energetic particle research. This is especially true in tokamaks where global modes can rapidly transport such particles away from the plasma core. Here stellarators appear have a natural advantage, as their three dimensional nature appears to suppress many of these modes [33]. In fact, codes developed to study such phenomena in stellarators are being applied to tokamaks to understand and predict mode suppression in tokamaks with 3D magnetic perturbations [34]. Inclusion of such codes in STELLOPT could help better constrain the optimization space in which energetic particle confinement can be improved.

2.4 Divertor Design

A fusion reactor requires a divertor and baffling geometry that can withstand the plasma particle and energy exhaust while enabling pumping of neutral particles, including helium created from fusion reactions. The system must also have acceptable sputtering properties, which depends on the plasma facing material choice and the self-consistent particle fluxes, to provide a satisfactory component lifetime and impurity influx into the core. Historically, stellarators have either operated without an explicit divertor structure (acceptable due to low input power and fluxes), or had a divertor designed after the magnetic configuration and coil geometry had been fixed. This process can cause issues due to limited space and the overload of components during the plasma evolution, issues that could potentially be avoided if the divertor design was included in the optimization procedure that produced the plasma and coil shapes. The in-

teraction between edge effects, such as sputtering, a strongly dissipative scrape-off-layer, and impurity transport cannot be decoupled from core confinement and must be addressed.

Tokamak reactors have largely settled on the poloidal divertor design, which cleanly separates the plasma into core, scrape-off layer, and private regions. The poloidal divertor has well-documented advantages and disadvantages over a limited configuration [35]. This concept has a natural analogue in a 3D system in the island divertor [36], where the edge transform is configured to provide a resonant value at the plasma edge, and the resulting island chain is intersected by PFCs. Optimized stellarators also tend to exhibit natural striated patterns of flux mapped from the last closed flux surface (LCFS) to an enclosing shape, exhibiting characteristics determined by the shape of the LCFS [37, 38]. The divertor fluxes and components are inherently three-dimensional in stellarators, which makes numerical optimization challenging. However, these two categories of divertor configuration have the advantage of providing well-defined flux patterns (for reasonable PFC geometry) that are robust to small changes in the ideal magnetic field definition. Resonant error fields can cause major modifications in the predicted heat fluxes [40], and must be minimized in all devices.

Ultimately the divertor design must be an integral part of the full-device optimization, with cost parameters that feed into the design of the coil system and the transport parametrization, which in turn affects the calculation of the divertor loads. As a first step, inclusion of divertor design in stellarator optimization involves including codes that can calculate heat loads onto arbitrary component geometry for 3D magnetic into the STELLOPT code along with their associated figures of merit. The simplest tool for this purpose is the use of magnetic field line tracing with cross-field diffusion that allows power to be mapped from the LCFS to the PFCs. This method has the advantage of being an embarrassingly parallelizable problem, and was im-

plemented in the DIV3D code, which was used to design the W7-X divertor scraper elements [39]. Similar methods have been implemented in other code packages, including FIELDLINES [31] and [40]. STELLOPT is built around magnetic equilibria calculated using the ideal nonlinear MHD code VMEC, which assumes the existence of nested closed flux surfaces. As such it does not provide fields to the PFCs (except in limiter configurations). To extend the fields outside of the VMEC domain a secondary calculation is required, which accounts for the magnetic fields generated by the equilibrium currents inside of the VMEC boundary. This extension is typically performed using a virtual-casing method [41, 42, 43, 44].

In the DIV3D code, the power loads are calculated by assuming that the heat transport is described by free-streaming parallel convection with random-walk cross-field diffusion. This model is implemented by initiating a large number of field lines randomly assigned over a flux surface inside the magnetic separatrix in a parallelized implementation. The field lines are traced in both directions, with randomly directed perpendicular steps of size Δ_{\perp} introduced corresponding to a magnetic diffusivity $D_m = (\Delta_{\perp})^2/\Delta_{\parallel}$, where Δ_{\parallel} is the step size parallel to the magnetic field used when integrating the field line differential equation. The magnetic diffusivity is a free parameter related to plasma transport quantities as χ_{\perp}/v , where χ_{\perp} is the thermal diffusivity and v the particle velocity. Generally, increasing D_m will result in broader flux patterns (width $\sim D_m^{1/2}$) and a decreased peak heat flux ($Q_{max} \sim D_m^{-1/2}$). The surface of each PFC is subdivided into a set of triangular facets, and the field lines are traced until an intersection with a facet is found. To convert the resulting strike patterns into a heat flux an equal fraction of the input power is assigned to each field line. The total power to each facet is divided by its area to calculate the heat flux.

Optimization of a component is achieved by specifying an initial shape, as well as a cost

function that is evaluated while manipulating the surface shape in three dimensions. In a stellarator design, the initial shape could come from expanding the LCFS, calculating the initial flux patterns, then defining poloidally and toroidally discrete shapes that encompass them. To decrease the computational time, a minimum number of triangular facets are used in the initial calculations, with the geometric fidelity increasing with the complexity of the component. The cost function should include engineering constraints, such as the minimum curvature space for cooling and support structure. These considerations were made when designing the W7-X scraper elements, highlighting the difficulty of simultaneously balancing plasma physics goals and engineering constraints. A highly shaped PFC can be designed that minimizes the incident flux, but this can come at great engineering complexity and cost. To facilitate the more advanced aspects of the design, e.g., fluid dynamics (cooling water pressure drop and temperature rise), and engineering constraints the optimization procedure should interface with CAD codes. A simple realization has been implemented in DIV3D, which reads in a CAD surface, calculates the heat flux and returns a new optimal surface in a format that can be imported into a CAD model. An example of this type of calculation is shown in Figure 8.

The type of heat flux calculation described above is simplistic, but would still represent an advancement stellarator optimization. Successive improvements to this estimate include incorporating a 1D transport model to individual flux tubes which accounts for parallel pressure gradients and a full 3D fluid plasma transport calculation, such as that performed by the EMC3-EIRENE code. A more much more complete model of edge transport is incorporated in the EMC3-EIRENE code [45, 46] which couples Monte-Carlo based fluid plasma transport (EMC3) to kinetic neutral particle transport and plasma surface interactions (EIRENE). As compared to the simple field line diffusion model EMC3-EIRENE accounts for many additional

important effects, including parallel diffusion and finite ν , plasma-neutral interactions and impurity radiation, all of which tend to decrease the predicted heat flux. EMC3-EIRENE also allows for the simulation of neutral particle transport and for the neutral pressure and pumping requirements to be directly calculated. The increased fidelity of EMC3-EIRENE comes at the cost of a greatly increased complexity in setting up a simulation, as well as an increased computational time.

Significant work remains in the definition and implementation of cost functions related to the plasma physics parameters. Using the toolset described above, a first-order model should consider maximization of the connection length L_c in wetted areas minimizing extrema in L_c and heat flux in the local distributions. This will reduce the convective component of the heat flux and increase the ability to have radiative dissipation along flux tubes, facilitating detachment. Avoidance of component edge wedging and tile gaps (eliminate leading edges), and reduce sensitivity to component positioning and alignment. These effects can be calculated first with field line diffusion, then refined with higher fidelity models. The use of more advanced transport solvers will allow for the inclusion of baffling for neutral particle guidance and maximization of neutral pressure in pumping regions. As a first estimate, these aspects can be calculated analytically [47]. As these plasma physics cost functions, and the engineering aspects are implanted, the relative weight factors as compared to the magnetic field, coil, and transport terms must be carefully tuned.

3. Summary

The objective of stellarator optimization is to address gaps in developing the stellarator concept as a reactor. This paper has summarized the following topics:

Simplification of stellarator magnets which allow improved maintenance access

Development of experimental scenarios for validating turbulence computations in stellarators to gain confidence in using turbulence optimization as a design criterion

Creation of tools and designs for achieving reactor-relevant alpha particle confinement

Mitigation of the materials challenge by integrating divertor design into the framework of stellarator optimization.

Successful inclusion of these optimization concepts as part of a concerted design effort could help solve many of the problems of fusion energy development.

References

- [1] H. E. Mynick, *Phys. Plasmas* **13** (2006) 058102.
- [2] A. H. Boozer, *Phys. Fluids* **23** (1980) 904.
- [3] A. H. Boozer, *Phys. Fluids* **26** (1983) 496.
- [4] Nuhrenberg and Zille, *Phys. Lett. A* **129** (1988) 113.
- [5] G. Y. Fu, et al., *Phys. Plasmas* **7** (2000) 1809.
- [6] W. A. Cooper, *Phys. Plasmas* **7** (2000) 2546.
- [7] D. A. Spong et al., *Nucl. Fusion* **41** (2001) 711.
- [8] T. Brown, et al., 2015 IEEE 26th Symposium on Fusion Engineering (SOFE),
10.1109/SOFE.2015.7482426
- [9] L.P. Ku, et al., *Fusion Science and Technology* **54** (2008) 673.

- [10] L.P. Ku and A. Boozer, Nucl. Fusion **50** (2010) 125005.
- [11] L. El-Guabaly, et al., Fus Sci Tech **54** (2008) 747.
- [12] V. V. Nemov, et al., Phys Plasmas **6** (1999) 4622.
- [13] M. Landreman, arXiv:1609.04378 (2016).
- [14] M. Landreman and A. H. Boozer, Physics of Plasmas **23** (2016) 032506.
- [15] P. C. Hansen, ?Rank-Deficient and Discrete Ill-Posed Problems,? SIAM (1998)
- [16] P. C. Hansen, J. G. Nagy, and D. P. O’Leary, ?Deblurring images,? SIAM (2006)
- [17] J. Chamorro-Servent et al., Opt. Express **19**, (2011) 11490.
- [18] V. Taroudaki and D. P. O’Leary, SIAM J. Sci. Comp. **37**, (2015) A2947.
- [19] M. Nunami, et al., Plasma Fusion Res **5** (2010) 16.
- [20] F. Jenko, et al., Physics of Plasmas **7** (2000) 1904.
- [21] J. Baumgaertel, et al., Phys. Plasmas **20** (2013) 022305.
- [22] J. H. E. Proll, et al., Phys. Rev. Letters **108** (2012) 245002.
- [23] P. Xanthopoulos, et al., Phys. Rev. X **6** (2016) 021033.
- [24] H. E. Mynick, Phys. Rev. Letters **105** (2010) 095004.
- [25] H. E. Mynick, et al., Phys. Plasmas **18** (2011) 056101.
- [26] H. E. Mynick, et al., Plas. Physics Control. Fusion **56** (2014) 094001.
- [27] P. Xanthopoulos, et al., Phys. Rev.Letters **113** (2014) 155001.

- [28] W. Lotz, et al., *Plas. Physics Control. Fusion* **34** (1992) 1037.
- [29] G. Grieger, et al., *Phys. Fluids B* **4** (1992) 2081.
- [30] F. Najmabadi and the ARIES-CS Team, *Fusion Science and Technology* **54** (2008) 655.
- [31] M. McMillan and S. A. Lazerson, *Plasma Phys. Control. Fusion* **56** (2014) 095019.
- [32] S. A. Lazerson, et al. in proceedings of the European Physical Society (2015).
- [33] D. A. Spong, R. Sanchez, and A. Weller, *Phys. Plasmas* **10** (2003) 3217.
- [34] G. J. Kramer, et al., *Plasma Phys. Control. Fusion* **58** (2016) 085003.
- [35] P.C. Stangeby, “The Plasma Boundary of Magnetic Fusion Devices”, Chapter 26, IOP Publishing, Bristol UK (2000).
- [36] Y. Feng, M. Kobayashi, T. Lunt, and D Reiter, *Plasma Phys. Control. Fusion* **53** (2011) 024009.
- [37] J. Nuehrenberg and E. Strumberger, *Contrib. Plasma Phys.* **32** (1992) 204.
- [38] A.H. Boozer, *J. Plasma Phys.* **81** (2015) 515810606.
- [39] J.D. Lore, et al., *Trans. Plasma Sci.* **42** (2014) 539.
- [40] S. A. Bozhenkov, et al., *Fusion Eng. Des.* **88** (2013) 2997.
- [41] V.D. Shafranov and L.E. Zakharov, *Nucl. Fusion* **12** (1972) 599.
- [42] E. Strumberger, *Nucl. Fusion* **37** (1997) 19.
- [43] M. Drevlak, D. Monticello and A. Reiman, *Nucl. Fusion* **45** (2005) 731.

[44] J. Geiger, et al., *Contrib. Plasma Phys.* **50** (2010) 770.

[45] Y. Feng, F. Sardei, J. Kisslinger, P. Grigull, *J. Nucl. Mater.* **241** (1997) 930.

[46] Y. Feng, F Sardei, J Kisslinger, *J. Nucl. Mater.* **266** (1999) 812.

[47] R. Maingi, J.G. Watkins, M.A. Mahdavi and L.W. Owen, *Nucl. Fusion* **39** (1999) 1187.

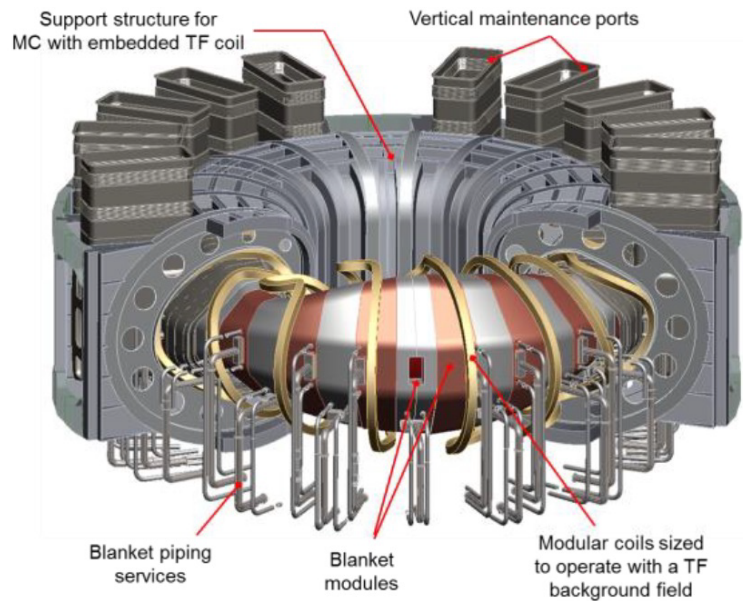


Figure 1: Cut-away view of a maintainable stellarator with the outer half of the modular coils constrained to be vertical for sector maintenance access.

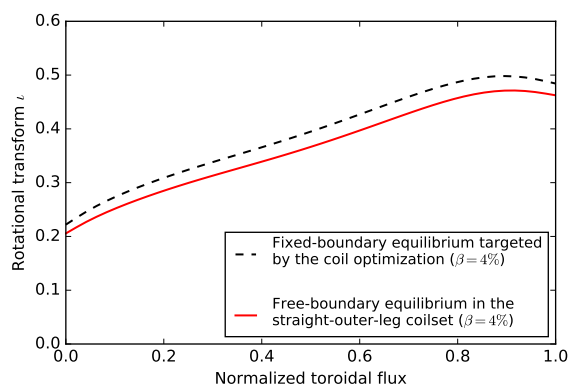


Figure 2: Rotational transform profile for the plasma configuration of Figure 1.

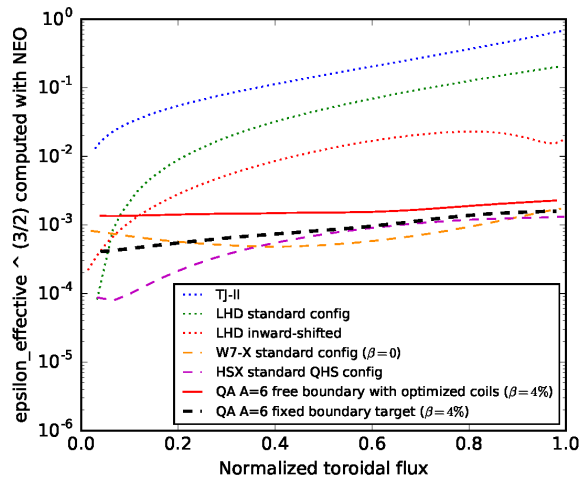


Figure 3: Normalized neoclassical transport for the plasma configuration of figure 1 (thick red solid curve and thick black dashed curve), with comparisons to other stellarators.

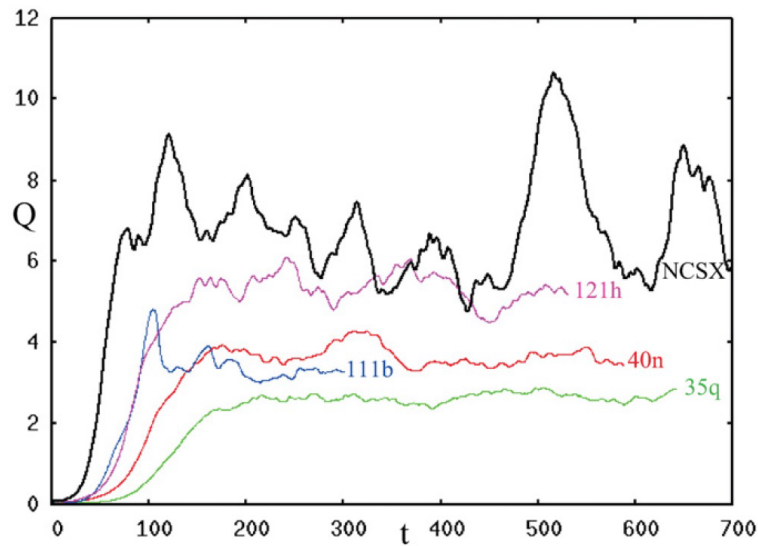


Figure 4: [From H. Mynick, et al., Plasma Phys. Control. Fusion **56** (2014) 094001] Averaged heat flux Q_gk versus time from nonlinear GENE runs for NCSX (black) and several turbulence-reduced QA systems

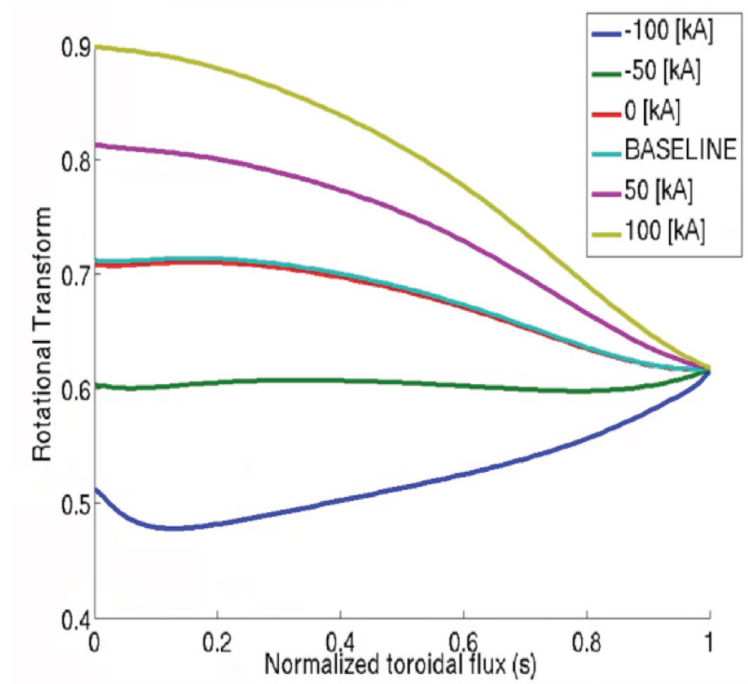


Figure 5: iota profiles for QUASAR shear scan. Legend indicates current in toroidal field coils.

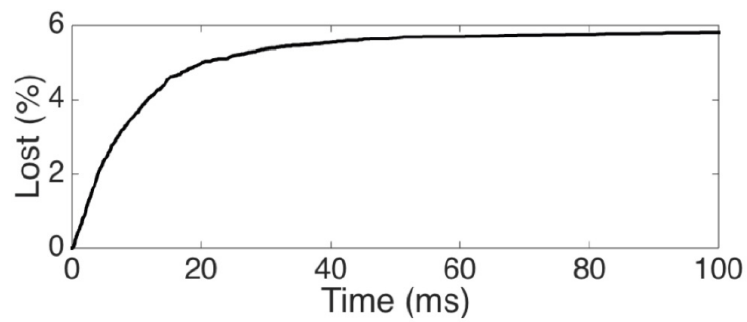


Figure 6: Particle loss fraction as a function of time as calculated by the BEAMS3D code.

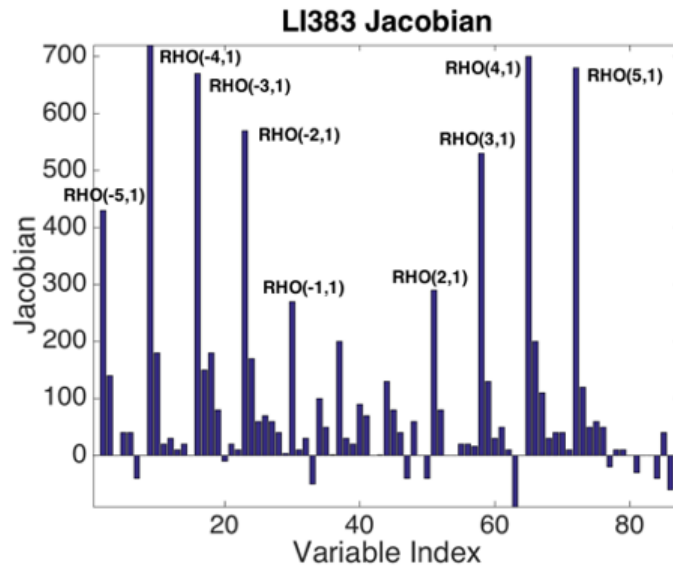


Figure 7: Shape space Jacobian of energetic particle confinement showing the relative effect of low order toroidal modes on losses.

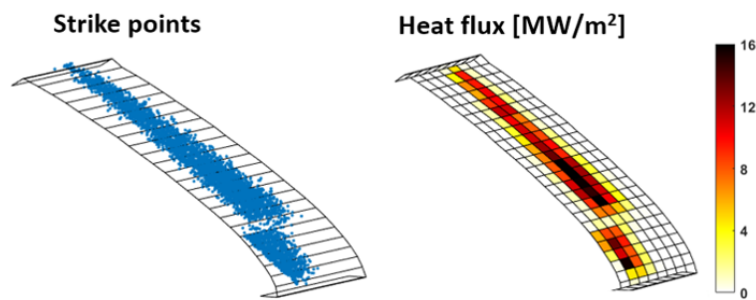


Figure 8: Calculation of strike points and simulated heat flux on the W7-X scraper element done using the DIV3D code.

Princeton Plasma Physics Laboratory Office of Reports and Publications

Managed by
Princeton University

under contract with the
U.S. Department of Energy
(DE-AC02-09CH11466)

P.O. Box 451, Princeton, NJ 08543
Phone: 609-243-2245
Fax: 609-243-2751

E-mail: publications@pppl.gov

Website: <http://www.pppl.gov>